Chromophore Aspartate Oxidation−Decarboxylation in the Green-to-Red Conversion of a Fluorescent Protein from *Zoanthus* sp. 2[†]

Alexey A. Pakhomov and Vladimir I. Martynov*

Shemyakin-Ovchinnikov Institute of Bioorganic Chemistry, Russian Academy of Sciences, Miklukho-Maklaya 16/10, 117997 Moscow, Russia

Received April 17, 2007; Revised Manuscript Received August 7, 2007

ABSTRACT: The red fluorescence of a *Discosoma* coral protein is the result of an additional autocatalytic oxidation of a green fluorescent protein (GFP)-like chromophore. This reaction creates an extra π-electron conjugation by forming a C═N−C═O substituent. Here we show that the red fluorescence of a protein from *Zoanthus* sp. 2 (z2FP574) arises from a coupled oxidation−decarboxylation of Asp-66, the first amino acid of the chromophore-precursory DYG sequence. Comparative mutagenesis of highly homologous green (zFP506) and red (z2FP574) fluorescent proteins from *Zoanthus* species reveals that an aspartate at position 66 is critical for the development of red fluorescence. The maturation kinetics of wild-type z2FP574 and the zFP506 N66D mutant indicates that the "green" GFP-like form is the actual intermediate in producing the red species. Furthermore, via maturation kinetics analysis of zFP506 N66D, combined with mass spectrometry, we determined that the oxidation−decarboxylation of Asp-66 occurs without detectable intermediate products. According to mass spectral data, the minor "red" chromophore of the z2FP574 D66E mutant appears to be oxidized and completely decarboxylation deficient, indicating that the side chain length of acidic amino acid 66 is critical in controlling efficient oxidation−decarboxylation. Substitutions with aspartate at the equivalent positions of a *Condylactis gigantea* purple chromoprotein and *Dendronephthya* sp. green fluorescent protein imply that additional oxidation of a GFP-like structure is a prerequisite for chromophore decarboxylation. In summary, these results lead to a mechanism that is related to the chemistry of β-keto acid decarboxylation.

Green fluorescent protein-like proteins from marine organisms span most of the visible spectrum, their diverse fluorescent colors being genetically encoded. Together, these properties enable extensive applications of green fluorescent protein-like proteins as imaging tools in molecular and cellular biology (*1*, *2*). A vital question in the biochemistry of green fluorescent protein-like proteins involves the mechanisms by which they tune their absorbance and/or fluorescence to a definite wavelength. Protein self-tuning within a wide spectral range is of particular interest, since this property is acquired by a rather conservative chemical mechanism. The proteins of the GFP[1] family contain a highly conserved XYG chromophore-forming amino acid sequence. After polypeptide folding, the protein matures via consecutive autocatalytic reactions within the internal XYG tripeptide. These reactions create a chromophore that includes a GFP-like structure as a principal building block. Currently, the diverse protein spectral properties are considered to be mainly due to additional chemical modifications of a GFP core structure, and these post-translational modifications apparently account for the protein coarse tuning. Further fine-tuning arises from different noncovalent interactions of the chromophore with its surroundings, which influence electron density or charge distribution along the chromophore π-system.

The customary post-translational modification of a GFP structure is an additional oxidation (presumably oxygen-mediated dehydrogenation). This reaction yields an acylimine substituent (C═N−C═O) in the polypeptide backbone, which extends π-system conjugation of a GFP structure (*3*). The resulting acylimine substituent accounts for the red shift in emission/absorbance spectra of some fluorescent proteins (FPs) and nonfluorescent chromoproteins (CPs) (*4*−*9*). The red-emitting protein z2FP574 (zoan2RFP), isolated from *Zoanthus* sp. 2 (*10*), exhibits fluorescence spectra very similar to that of the red fluorescent protein from *Discosoma* sp. (DsRed), with excitation and emission maxima at 552 and 574 nm for z2FP574 and 558 and 583 nm for DsRed. The recently determined crystal structure of z2FP574 (zRFP574) revealed a novel post-translational modification resulting in decarboxylation of the first amino acid of the Asp-Tyr-Gly chromophore-forming sequence (*11*). These findings raise the question of whether the decarboxylation is critical to the z2FP574 red shift acquisition and whether the red fluorescence of DsRed and z2FP574 is attained by different chemical mechanisms.

[†] This work was supported by the Russian Foundation for Basic Research (06-04-48196) and by a grant from the Russian Academy of Sciences for the program "Molecular and Cellular Biology" (200101).

* To whom correspondence should be addressed. Telephone: 7(495) 336-5111. Fax: 7(495) 335-7103. E-mail: vimart@list.ru.

[1] Abbreviations: FP, fluorescent protein; CP, chromoprotein; GFP, green fluorescent protein from *Aequorea victoria*; DsRed, red fluorescent protein from *Discosoma* sp.; cgCP, purple chromoprotein from *Condylactis gigantea*; zFP506, green fluorescent protein from *Zoanthus* sp.; z2FP574, red fluorescent protein from *Zoanthus* sp. 2; ESI, electrospray ionization; TOF MS, time-of-flight mass spectrometry; rms, root-mean-square.

10.1021/bi700721x CCC: $37.00
Published on Web 09/25/2007

Here, we demonstrate that the red fluorescence of z2FP574 is the result of a coupled oxidation−decarboxylation of a GFP-like chromophore. Comparative mutational analysis of z2FP574 and a green fluorescent protein, zFP506, suggests a key role for the first chromophore-forming amino acid in z2FP574's red fluorescence acquisition. We further create mutations that substantially decelerate the "red" chromophore synthesis and analyze the reaction products by mass spectrometry. Altogether, the obtained results suggest a mechanism similar to that of β-keto acid decarboxylation.

MATERIALS AND METHODS

Protein Expression, Purification, and Mutagenesis. The plasmids pQE30-z2FP574 and pQE30-zFP506 were a generous gift from K. A. Lukyanov (Shemyakin-Ovchinnikov Institute of Bioorganic Chemistry, Russian Academy of Sciences). Recombinant proteins containing an N-terminal polyhistidine tag were expressed in *Escherichia coli* and purified from cell lysates by metal-affinity chromatography on Ni-NTA resin (Qiagen) according to the manufacturer's protocol. Site-directed mutagenesis was performed with the QuikChange site-directed mutagenesis kit (Stratagene). The resulting plasmids were sequenced to verify mutations.

Optical Spectroscopy. To measure absorbance spectra, after Ni-NTA chromatography the samples were exchanged into a buffer of 20 mM sodium phosphate and 150 mM NaCl (pH 7.0). Absorbance was measured using a Cary 50 Bio UV/vis spectrophotometer (Varian). The fluorescence measurements were carried out using a Varian Cary Eclipse fluorescence spectrophotometer. For wild-type z2FP574 maturation kinetics measurements, freshly transformed *E. coli* cells were grown in 200 mL of LB broth containing 100 μg/mL ampicillin overnight at 37 °C (under these conditions, the protein maturation is usually far from completion). The cells were further suspended in a buffer of 20 mM sodium phosphate and 150 mM NaCl (pH 7.0) and disrupted by sonication. Recombinant proteins were quickly purified from the soluble fraction by Ni-NTA chromatography. A solution of 0.1 M EDTA in the starting buffer was used for an immediate and complete elution; protein samples were not further buffer exchanged in this case. Absorption spectra of maturing proteins were collected at room temperature (22 °C). An elevated 280 nm absorbance is always observed for the samples eluted by EDTA (Figure 3A), which is apparently due to the admixed Ni^{2+}−EDTA complex. For COPASI simulation, the absorbance at 280 nm was used to determine protein concentrations (*12*), taking into account the known amino acid content. The extinction coefficient at 552 nm of the red form (R) was calculated from the absorbance ratio at 552 and 280 nm after extensive dialysis of the mature protein ($A_{552}/A_{280} = 2.01$; $\epsilon_{552} = 68\,300$). The extinction coefficient at 490 nm of z2FP574 D66A calculated by the same method ($\epsilon_{490} = 78\,100$) was utilized to determine concentrations of the intermediate green form (G) of wild-type z2FP574.

Chromopeptide Isolation and Mass Spectrometry. Wild-type z2FP574 was denatured by addition of a NaOH solution to a final concentration of 0.15 M. The protein solution was further complemented with Tris (10 mM) and titrated with hydrochloric acid to pH 7.8. Chymotrypsin (Sigma) digestion [enzyme-to-protein ratio of 1:30 (w/w)] was performed at 37 °C overnight and finally quenched with acetic acid (to pH 4.0). Mutant proteins were denatured by addition of a 0.1 M HCl solution to a final pH of 2.3. According to SDS−PAGE (Figure 1 of the Supporting Information, shown for cgCP A63D), under these conditions the polypeptide chain was not significantly cleaved due to the acylimine hydrolysis. Pepsin (Sigma) was then added in a 1:30 (w/w) ratio, and digestion was carried out at room temperature for 24 h. Digests were applied onto a reverse phase HPLC column (Beckman Ultrasphere ODS) equilibrated with 10 mM sodium phosphate buffer (pH 4.0), and peptides were eluted via a linear gradient of acetonitrile in the same buffer. The effluent was monitored at 210 and 380 nm. Peptides absorbing at 380 nm were collected and analyzed by MS. A Bruker Daltonics Esquire 3000 Plus mass spectrometer equipped with an electrospray source of ionization and ion trap analyzer was used for mass spectral analysis of the wild-type z2FP574 chromophore-bearing peptide. The peptide was injected in a 0.1% formic acid, 50% methanol solution at a flow rate of 1.5 μL/min. Peptides from mutant proteins were analyzed with a Bruker Daltonics Ultraflex MALDI-TOF/TOF mass spectrometer using α-cyano-4-hydroxycinnamic acid (Bruker) as a matrix.

RESULTS

Mass Spectral Analysis of the Wild-Type z2FP574 Chromophore-Bearing Peptide. Given that aspartate and glutamate residues are sometimes susceptible to X-ray-induced decarboxylation (*13*), we examined the recently reported z2FP574 (zRFP574) crystal structure data for the chromophore post-translational modifications described therein (*11*). To this end, completely mature wild-type z2FP574 was subjected to denaturation, followed by chymotrypsin digestion. The chromophore-containing peptide absorbing at 380 nm was isolated by HPLC. Amino acid sequencing revealed that a Ser-Ala-Ala- fragment is the N-terminal sequence of the chromopeptide. The ESI ion trap mass spectrum of the isolated chromopeptide exhibited a major +1 charged peak at *m*/*z* 1194.6. This *m*/*z* value is consistent with a modified SAAF***DYG***NRLF (*10*) peptide containing a GFP-like core unit (mass loss of 20 Da, as compared to the mass of a parent unmodified peptide) that has lost an additional 46 Da. These data suggested an additional dehydrogenation (oxidation) and decarboxylation of a GFP core structure. Further fragmentation of the chromopeptide ion using tandem mass spectrometry generated carboxy-terminal (x, y, z) and amino-terminal (a, b, c) ions with *m*/*z* values consistent with the peptide sequence described above (Table 1). Furthermore, comparative analysis of the peaks at *m*/*z* 801.4 (z_7) and 777.3 (x_6 + 2H) showed that the z2FP574 chromophore had undergone an additional oxidation−decarboxylation at Asp-66 (Figure 1A) proposed previously by crystallographic studies of the intact protein (*11*). It has recently been reported that illumination of GFP results in phototransformation of the protein and leads to oxidative decarboxylation of a glutamate residue, which is in the vicinity of the chromophore [the Glu-222 residue is equivalent to Glu-221 in z2FP574 (Figure 1B)] (*14*). To test whether the z2FP574 red chromophore synthesis and decarboxylation of Asp-66 depends on light, maturation of wild-type z2FP574 was carried out in the dark. The dark-mature protein showed absorbance and fluorescence spectra indistinguishable from those of the protein that matured in

Table 1: Experimental[a] and Calculated *m*/*z* Values of the Fragment Ions Derived from the Wild-Type z2FP574 Chromopeptide Ion in the Secondary Mass Spectrum

ion	*m*/*z* (observed)	*m*/*z* (calcd)	relative amplitude
a_9	888.4	888.4	1
b_9	916.4	916.4	19
a_{10}	1001.4	1001.5	5
b_{10}	1029.4	1029.5	23
b_{11}	1176.5	1176.6	22
z_3	418.2	418.2	1
y_4	549.3	549.3	1
z_4	532.3	532.3	3
$x_6 + 2H$	777.3	777.3	9
y_7	818.4	818.4	24
z_7	801.4	801.4	100
y_8	965.4	965.4	3
y_9	1036.4	1036.5	4
y_{10}	1107.5	1107.5	1
z_{11}	1177.5	1177.5	33

[a] The wild-type SAAF***DYG***NRLF chromopeptide ion (parent at *m*/*z* 1194.6) was subjected to collisional fragmentation. The observed *m*/*z* reduction of 66 units, as compared with that of the unmodified fragment sequence, is consistent with a cyclization reaction (dehydration), two sites of dehydrogenation, and decarboxylation. An *m*/*z* loss of 20 units of the chromophore-bearing fragments is consistent with the cyclization reaction and one site of dehydrogenation.

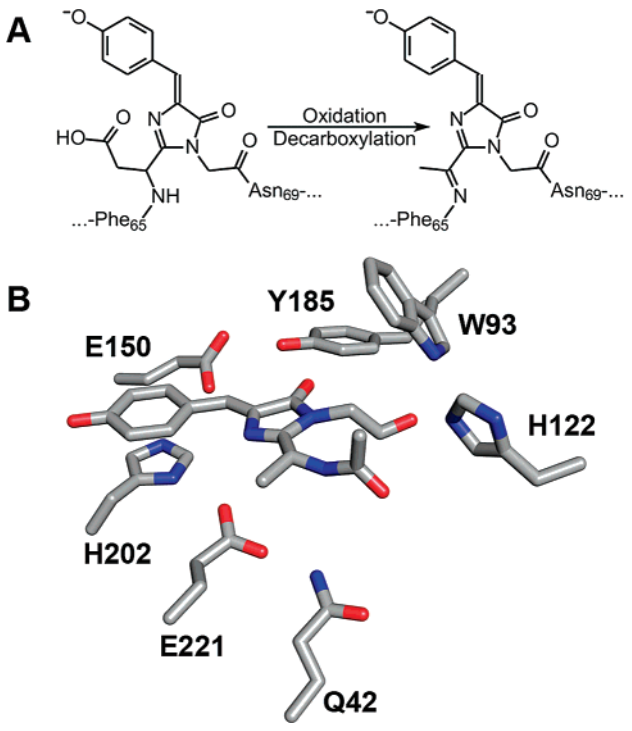

FIGURE 1: Schematic outline of proposed chromophore-forming reactions and chromophore environments in wild-type z2FP574. (A) Proposed oxidation−decarboxylation of a GFP-like chromophore-precursory structure in the course of wild-type z2FP574 maturation. (B) Three-dimensional structure illustrating z2FP574 chromophore environments [zRFP574, PDB entry 2FL1 (*11*)]. The sequence alignment predicts chromophore environments in green fluorescent protein, zFP506, and red fluorescent protein, z2FP574, to be quite similar. The first chromophore-forming amino acid of zFP506 is Asn-66. Oxygen atoms are colored red and nitrogen atoms blue.

daylight. Dark-mature z2FP574 was digested by chymotrypsin, and the chromophore-bearing peptide was isolated by HPLC. The ESI mass spectrum of the isolated chromopeptide contained a +1 charged peak at *m*/*z* 1194.6, indicating that additional oxidation and decarboxylation of chromophore Asp-66 are light-independent reactions.

Comparative Mutational Analysis of z2FP574 and zFP506 at Position 66. Comparative sequence analysis of a green fluorescent protein from *Zoanthus* sp., zFP506, and a red fluorescent protein from *Zoanthus* sp. 2 (*10*), z2FP574, revealed 84% amino acid identity. The crystal structure of z2FP574 (*11*) and sequence alignment predicted a striking similarity in the immediate environment of the zFP506 and z2FP574 chromophores. This analysis revealed only one significant difference at position 66, the first position of the chromophore-forming tripeptide, which is occupied by Asn and Asp in zFP506 and z2FP574, respectively (Figure 1B, shown for z2FP574). To study the importance of amino acid 66 with respect to the red fluorescence, we introduced substitutions at this position in both zFP506 and z2FP574. The consequences of mutations were tested both by optical spectroscopy and by mass spectral analysis of the corresponding isolated chromopeptides.

Since oxidation and decarboxylation of Asp-66 in z2FP574 lead to the formation of Cα,N-dehydroalanine (Figure 1A), we substituted alanine for aspartate in z2FP574 to test whether the side chain carboxyl is essential for the oxidation reaction. D66A exhibited an absorbance maximum shift to 490 nm and green emission of the protein. Mass spectra of the chromopeptide isolated from the pepsin digest showed the *m*/*z* 1049.5 peak, consistent with the GFP-like chromophore structure within a SAAF***AYG***NRL peptide. Like D66A, the D66N variant also exhibited green emission. Mass spectra of the D66N chromopeptide contained an *m*/*z* 1092.5 peak, consistent with a GFP-type chromophore within a SAAF***NYG***NRL peptide. These results clearly indicate that oxidation at position 66 is somehow dependent on the decarboxylation of a carboxyl moiety in the side chain of amino acid 66.

We further tested the impact of the side chain length of acidic amino acid 66 on decarboxylation. Insertion of an additional methylene group into the side chain by the D66E substitution within z2FP574 led to a major component of green emission (excitation and emission maxima at 490 and 506 nm, respectively), with a relatively weak residual red fluorescence (excitation maxima at 490 and 552 nm and emission maximum at 570 nm). After maturation for 4 days at 37 °C, the D66E mutant showed a major peak of a 490 nm-absorbing green form and a small peak of a 552 nm-absorbing red species. The red-to-green absorbance ratio did not increase beyond the extent shown in Figure 2A upon prolonged incubation or at elevated temperatures. The D66E mutant was digested by pepsin, and chromopeptides corresponding to both green and red species were isolated by HPLC. Mass spectra of a green chromopeptide contained the *m*/*z* 1107.5 peak, whereas the red chromophore-bearing peptide exhibited the *m*/*z* 1105.5 peak, indicating additional dehydrogenation of a GFP-like structure within a SAAF***EYG***NRL peptide. The green and red species were further subjected to tandem mass spectrometry (Table 2), which showed that the chromophore glutamate of the minor red species is dehydrogenated and decarboxylation-deficient. These results suggested that the side chain length of acidic amino acid 66 is critical to decarboxylation; furthermore, D66A and D66N mutants suggested that decarboxylation promotes efficient oxidation at position 66. To examine the importance of

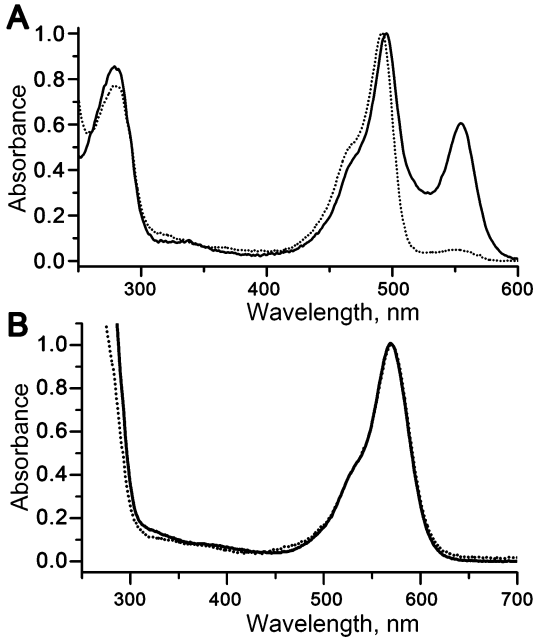

FIGURE 2: Absorbance spectra of mutant and wild-type proteins. (A) Normalized absorbance spectra of z2FP574 D66E (···) and zFP506 N66D (—). Spectra were recorded after protein maturation for 4 days at 37 °C. (B) Normalized absorbance spectra of wild-type cgCP (···) and cgCP A63D (—).

aspartate, we introduced an N66D substitution into a green fluorescent protein zFP506. Maturation of zFP506 N66D proved to be a highly temperature-sensitive process; above 30 °C, the zFP506 N66D mutant produced appreciable amounts of the red form with an absorbance maximum at 555 nm (Figure 2A). Mass spectra of the green and red chromopeptides isolated from the peptic digest of N66D showed *m*/*z* 1226.6 and 1180.6 peaks, respectively. These *m*/*z* values are consistent with the SAAF***DYG***NRVF peptide containing either a GFP-like green chromophore or a red one with an additionally oxidized and decarboxylated GFP-like structure. Tandem mass spectra of the red chromopeptide confirmed additional oxidation−decarboxylation at position 66 (Table 2).

Additional Oxidation of a GFP Core Structure Is Essential for Decarboxylation. An electron-deficient imidazolidinone ring of the avGFP chromophore was recently proposed to be an oxidizing moiety in oxidative decarboxylation of Glu-222 upon GFP phototransformation (*14*). We asked whether the chromophore imidazolidinone ring could act as an oxidant in oxidation−decarboxylation of Asp-66. The S65D substitution of avGFP yielded a protein that was essentially nonfluorescent; however, the H62D variant of Dend FP, the protein from *Dendronephthya* sp. (*15*), produced green fluorescence. Continuous 366 nm illumination or elevated temperatures did not affect the Dend FP H62D absorbance and fluorescence spectra. The MALDI-TOF mass spectrum of the chromopeptide isolated from the Dend FP H62D pepsin digest exhibited an *m*/*z* 1236.5 peak (the TTAL***DYG***NRVF peptide), consistent with an unmodified aspartate within a GFP-like chromophore. We next tested whether additional oxidation that leads to the acylimine substituent within a DsRed-like chromophore would promote aspartate decarboxylation. We have chosen a chromoprotein from *Condylactis gigantea*, since the nature of the first amino acid of the XYG chromophore-forming sequence of cgCP was shown to be dispensable for acylimine formation (*9*). The A63D mutant of cgCP exhibited an absorbance maximum at 571 nm, exactly the same as that of the wild-type protein (Figure 2B). The cgCP A63D variant was digested with pepsin, and the chromophore-bearing peptide was isolated by HPLC. The MALDI-TOF mass spectrum of the A63D chromopeptide contained two +1 charged peaks at *m*/*z* 994.3 and 1038.3 (Figure 2 of the Supporting Information). The first *m*/*z* value is exactly the same as that observed for the wild-type chromopeptide, SPCC***AYG***SKT (*9*), suggesting that aspartate within the cgCP A63D chromophore is oxidized and decarboxylated. The peak at *m*/*z* 1038.3 is consistent with a pre-decarboxylation acylimine-bearing intermediate.

The Green GFP-like Form Is an Intermediate in the Synthesis of the Red Chromophore. To improve our understanding of the synthesis of the red chromophore, we studied maturation kinetics of wild-type z2FP574 by following absorbance spectrum changes. Rapidly purified immature z2FP574 was incubated at 22 °C, and absorbance spectra were recorded at the selected time intervals (Figure 3A). At the early stages of maturation, absorbance scans showed a major component with a maximum at 505 nm, which is obviously due to the green anionic form of a GFP-like chromophore. Maximally absorbing at 552 nm with a shoulder at 517 nm, the red form of z2FP574 became dominant at later stages. The time course of absorbance development at 552 nm exhibited a sigmoid shape, suggesting that an intermediate species exists at the early stages of z2FP574 maturation (Figure 3B). Unlike DsRed, fully mature wild-type z2FP574 lacked any noticeable absorbance of the green form. At this stage of the experiment, we proceeded on the assumption that only green and red species contribute to the overall visible spectra. Therefore, the spectrum of a green constituent at a given time point was calculated by subtracting the spectrum of completely mature z2FP574 (prenormalized to the 552 nm absobance value of each absorbance scan) from the overall absorbance spectra. The time course of absorbance evolution at 505 nm (Figure 3B) was determined after this subtraction operation. The resulting curve implied that the green anionic form of a GFP-like chromophore might be an intermediate in the z2FP574 red chromophore synthesis. To test this reaction scheme, the obtained kinetic data were fitted to different kinetic models via a global curve fitting procedure. To this end, COPASI biochemical simulation software was applied (*16*). Irreversible reaction mass action type was employed, and reaction parameters were estimated by means of the Levenberg−Marquardt method. Four kinetic models were tested, each of them starting from the protein containing the spectrally undetectable colorless form (**C**). First, we analyzed a model in which **C** directly converts into a green form (**G**) and the **G** form directly converts into a red form (**C** → **G** → **R**). Second, we tested a model containing an intermediate (**I**) in the course of green-to-red conversion (**C** → **G** → **I** → **R**). Although a blue intermediate (408 nm) was not detected upon z2FP574 maturation, we tested a DsRed-like model, in which a **G** form was proposed to be a "dead-end" product (*17*). In this case, the time course of **G** and **R** form development of z2FP574 was fitted to a kinetic model similar to that of Verkhusha et al. (*17*). To distinguish between different kinetic models, the fits were evaluated via a comparison of

Table 2: Fragment Ions Detected in Secondary Mass Spectra of Green and Red Chromopeptides of z2FP574 D66E and zFP506 N66D[a]

z2FP574 D66E[b]					zFP506 N66D[c]				
ion	green *m/z* (calcd)	green *m/z* (observed)	red *m/z* (observed)	green − red *m/z*[d]	ion	green *m/z* (calcd)	green *m/z* (observed)	red *m/z* (observed)	green − red *m/z*[d]
a_7	678.3	678.3	676.4	1.9	c_6	652.2	652.1	606.2	45.9
b_7	706.3	706.3	704.3	2.0	a_7	664.3	664.2	618.1	46.1
a_8	792.3	792.3	790.3	2.0	c_8	823.3	823.4	777.3	46.1
b_8	820.3	820.3	818.3	2.0	a_9	934.4	934.3	888.4	45.9
a_9	948.4	948.4	946.4	2.0	b_9	962.4	962.4	916.4	46.0
b_9	976.4	976.4	974.4	2.0	a_{10}	1033.5	1033.5	987.5	46.0
a_{10}	1061.4	1061.4	1059.4	2.0	b_{11}	1208.5	1208.5	1162.4	46.1
b_{10}	1089.5	1089.4	1087.4	2.0	$x_6 + 2H$	763.3	763.1	763.3	−0.2
$x_5 + 2H$	630.3	630.2	630.2	0.0	y_7	850.4	850.3	804.4	45.9
y_6	731.3	731.3	729.3	2.0	z_7	833.4	833.2	787.4	45.8
z_6	714.3	714.3	712.2	2.1	y_8	997.4	997.5	951.5	46.0
y_7	878.4	878.4	876.3	2.1	z_8	980.4	980.4	934.4	46.0
z_7	891.4	891.4	889.3	2.1	y_9	1068.5	1068.4	1022.3	46.1
y_8	949.4	949.4	947.3	2.1	y_{10}	1139.5	1139.5	1093.5	46.0
z_8	932.4	932.4	930.4	2.0					
y_9	1020.5	1020.4	1018.4	2.0					

[a] The green and red chromopeptides were isolated from z2FP574 D66E (parent chromopeptide ions at *m/z* 1107.5 and 1105.5, respectively) and zFP506 N66D (parent ions at *m/z* 1226.6 and 1180.6, respectively) digests and separately subjected to collision-induced fragmentation. The table includes only the chromophore-bearing fragment ions. [b] Chromopeptide sequence of SAAF***EYG***NRL. [c] Chromopeptide sequence of SAAF***DYG***NRVF. [d] Green −red *m/z* represents the observed green vs red species fragment *m/z* difference.

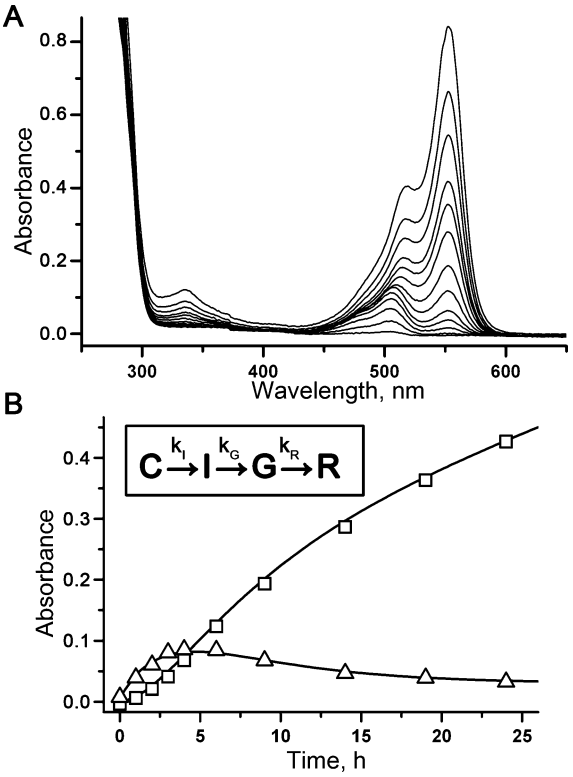

FIGURE 3: Absorbance evolution in the course of wild-type z2FP574 maturation. (A) Absorbance spectra were measured at different stages of z2FP574 maturation (0, 1, 2, 3, 4, 6, 9, 14, 19, 24, 35, 46, and 67 h after protein purification) at 22 °C (protein concentration of 0.45 mg/mL). (B) Time course of the absorbance development (0, 1, 2, 3, 4, 6, 9, 14, 19, and 24 h after protein purification) at 552 (□) and 505 nm (△). The spectrum of a green constituent at a given time point and absorbance development of the green form at 505 nm were calculated by subtracting the spectrum of completely mature z2FP574 (normalized to the 552 nm absobance value of each scan) from the overall absorbance spectra. The inset shows a proposed scheme for the consecutive reactions upon z2FP574 maturation. Solid lines represent simulated curves corresponding to the kinetic model shown in the inset.

the root-mean-square (rms) deviations of the simulated and experimental absorbance development curves (calculated extinction coefficients are presented in Materials and Methods). All three models described above showed unsatisfactory quality of fits for **G** and **R** forms, which was reflected in an elevated rms deviation. Finally, we tested a kinetic model with an intermediate (**I**) between **C** and **G** forms (**C** → **I** → **G** → **R**). The obtained kinetic data fitted this model significantly better with a rms deviation value of 0.009 (Figure 3B). An intermediate **I** was not detected experimentally, due to the lack of absorbance in the visible region (probably cyclized and not yet oxidized chromophore). However, elimination of **I** from the reaction pathway (**C** → **G** → **R**) led to a considerable rms deviation increase (0.036). The rate constants for this model were as follows: $k_{\mathbf{I}} = (1.4 \pm 0.5) \times 10^{-6}$ s^{-1}, $k_{\mathbf{G}} = (5.2 \pm 0.6) \times 10^{-5}$ s^{-1}, and $k_{\mathbf{R}} = (9.1 \pm 0.3) \times 10^{-5}$ s^{-1} (reflecting $t_{1/2}$ values of 13.9, 3.7, and 2.1 h, respectively).

Further support for the green intermediate came from the analysis of the spectral transition of the N66D mutant of zFP506. In contrast to that of wild-type z2FP574, the synthesis of the red product of zFP506 N66D at temperatures below 30 °C was substantially decelerated. Absorbance and fluorescence spectra revealed that the N66D variant that matured at 4 °C is arrested at a green state, and completely devoid of the red form. However, the green form of zFP506 N66D is converted to the red one at elevated temperatures (Figure 4A). The isosbestic point at 514 nm suggested that a green-to-red reaction proceeds without the formation of long-lived intermediate species. We further investigated the chemistry of the green-to-red transition by mass spectrometry. The reaction was initiated by heating the solution to 50 °C and stopped in various time intervals by cooling an aliquot to 4 °C. The protein in an aliquot was further digested by pepsin, and the protein digest was analyzed by MALDI-TOF mass spectrometry. As expected, the initial green form exhibited an *m/z* 1226.6 peak corresponding to the chromopeptide mass with a GFP-like chromophore structure (Figure 4B,C). Along with the appearance of a 552 nm-absorbing peak in the course of the green-to-red transition, a peak at *m/z* 1180.6 was detected in the mass spectra,

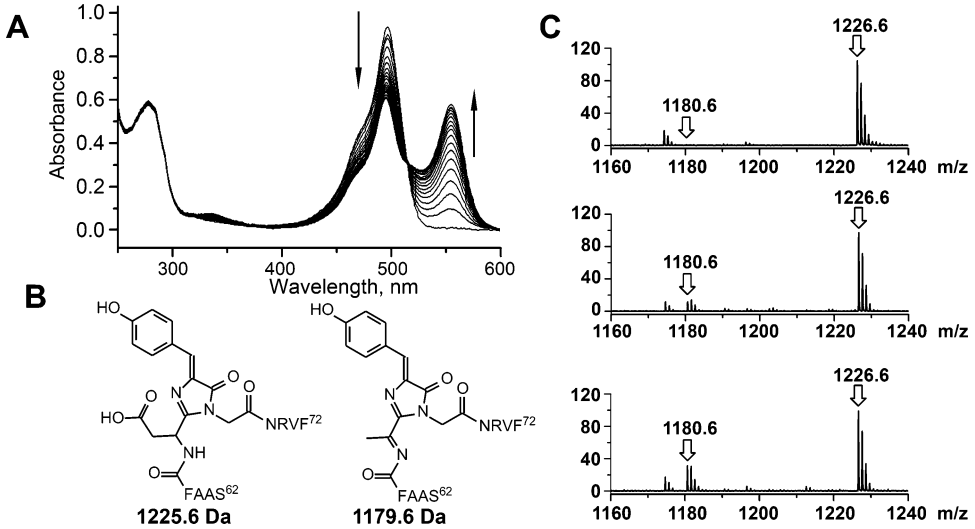

FIGURE 4: Green-to-red conversion of the zFP506 N66D mutant. (A) Kinetic series of the zFP506 N66D conversion at 50 °C. The spectra were recorded in 1 h intervals. (B) Proposed chromopeptide structures of zFP506 N66D green (left) and red (right) forms. The calculated mass values are presented below. (C) MALDI-TOF mass spectral changes in the course of the zFP506 N66D green-to-red conversion (spectra from top to bottom). The zFP506 N66D conversion results in a chromopeptide mass reduction of 46 Da. There are no detectable decarboxylated-only or oxidized-only intermediate products (mass loss of 44 or 2 Da, respectively). The reaction was initiated by heating the zFP506 N66D solution to 50 °C and stopped at various time intervals by cooling an aliquot to 4 °C. The protein in an aliquot was further digested by pepsin, and the protein digest was analyzed by MALDI-TOF mass spectrometry.

Table 3: Comparison of Spectral Properties and Chromophore Post-Translational Modifications of the Wild-Type and Mutant Proteins

protein	chromopeptide	protein absorbance maximum (nm)	observed chromopeptide (*m*/*z*)	mass loss[a] (Da)	modifications of the GFP chromophore[b]
wild-type z2FP574	SAAF*DYG*NRLF	552	1194.6	66	−2H, $-CO_2$
z2FP574 D66A	SAAF*AYG*NRL	490	1049.5	20	−
z2FP574 D66N	SAAF*NYG*NRL	491	1092.5	20	−
z2FP574 D66E[c]	SAAF*EYG*NRL	490	1107.5	20	−
		552	1105.5	22	−2H
zFP506 N66D[c]	SAAF*DYG*NRVF	496	1226.6	20	−
		555	1180.6	66	−2H, $-CO_2$
wild-type cgCP[d]	SPCC*AYG*SKT	571	994.4	22	−2H
cgCP A63D	SPCC*DYG*SKT	571	994.3	66	−2H, $-CO_2$
			1038.3	22	−2H
DendFP H62D	TTAL*DYG*NRVF	493	1236.5	20	−

[a] Total mass loss, as compared with that of the unmodified peptide with the same sequence. [b] Additional modifications of the chromophore GFP-core structure. [c] For z2FP574 D66E and zFP506 N66D, the data are given separately for the green and red species. [d] Optical properties and chromophore post-translational modifications reported for wild-type cgCP in ref *9*.

consistent with the loss of two protons (oxidation) and CO_2 by a GFP-like structure. According to the mass spectra, the green-to-red reaction products were deficient in decarboxylated-only or oxidized-only intermediate species (Figure 4B,C).

DISCUSSION

In red fluorescent proteins and chromoproteins, a GFP-like structure is further oxidized to the acylimine substituent (*3*−*9*, *18*), enabling additional extension of the chromophore π-electron system, and consequently leading to the red-shifted absorption and emission spectra. In this study, we established that the red fluorescence of z2FP574 is a result of a coupled oxidation−decarboxylation of Asp-66, reactions eventually yielding an acylimine substituent within the z2FP574 chromophore. Some properties of the wild-type and mutant proteins and interpretation of chromophore modifications are summarized in Table 3. Mass spectra of the chromopeptide isolated from z2FP574 showed it is 46 Da lighter than would be expected for a GFP-like chromophore. Tandem mass spectra unequivocally indicated this mass loss is due to an additional oxidation−decarboxylation of Asp-66 (Table 1 and Figure 1A), previously proposed in crystallographic studies of the intact protein (*11*). These results implied that some complementary mechanisms relevant to the z2FP574 red fluorescence acquisition may be in operation. First, we examined the possibility of the Kolbe mechanism, which has recently been proposed to be responsible for light-induced decarboxylation of the glutamate residue that is a neighbor of the GFP chromophore (*14*). Dark-mature z2FP574 underwent oxidation−decarboxylation of Asp-66 and displayed the same absorbance and fluorescence spectra as the protein that matured in daylight. These results suggested that oxidation and decarboxylation of the chromophore Asp-66 are light-independent reactions.

It has recently been reported that the nature of the first chromophore-forming amino acid of a chromoprotein from *C. gigantea* is dispensable for the protein's red shift development (*9*). The situation is quite different for the proteins from *Zoanthus* species. Remington et al. (*19*) demonstrated that substitutions at position 66 with aspartate or glutamate partially convert zFP538, a yellow fluorescent

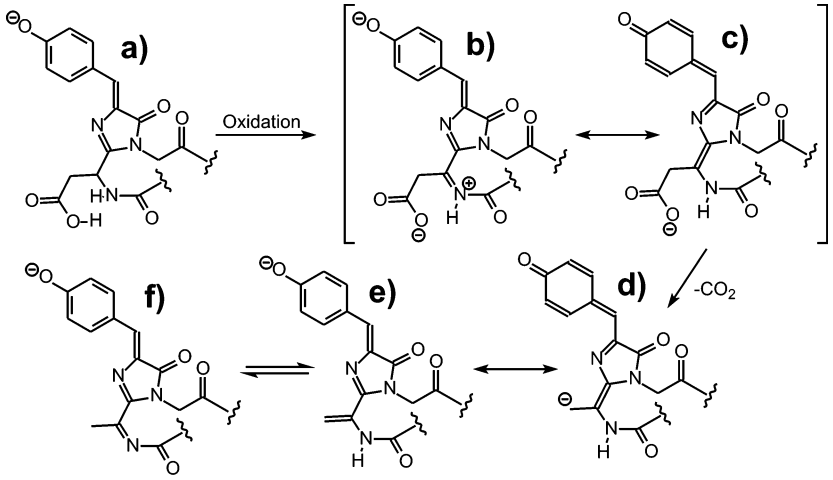

FIGURE 5: Proposed steps of z2FP574 chromophore formation. The green anionic form of a GFP-like chromophore is an intermediate (**a**) in the z2FP574 red chromophore synthesis (**f**).

protein from *Zoanthus* sp., into a red fluorescent protein. However, the chemical basis of this phenomenon has not been elucidated. By comparative mutational analysis of z2FP574 and zFP506 at position 66, and by mass spectral analysis of corresponding chromopeptides, we demonstrate that decarboxylation and efficient oxidation at position 66 are interrelated reactions (Table 3). To test whether the lack of a carboxy group in the side chain would influence oxidation, we introduced the D66N and D66A substitutions into wild-type z2FP574. The chromophore structure of D66N is nearly isosteric to the original green chromophore of the wild-type protein; however, asparagine would not be expected to decarboxylate. The D66A chromophore is isosteric to a hypothetic decarboxylated but not yet oxidized intermediate. Both z2FP574 D66N and D66A displayed green fluorescence and, according to mass spectra, failed to oxidize (Table 3). These results suggested that oxidation is somehow coupled with decarboxylation. To uncouple these reactions, we introduced the D66E mutation into z2FP574. In D66E, oxidation and decarboxylation sites are separated by an additional CH_2 spacer group. Despite the fact that the D66E mutant showed slight accumulation of the oxidized non-decarboxylated species, the yield of the oxidized red chromophore, as judged by the absorbance at 552 and 490 nm, was too low (Figure 2A). Therefore, it appeared that the decarboxylation reaction promotes efficient oxidation. We further constructed the N66D variant of a green fluorescent protein, zFP506, with the expectation that decarboxylation would be less facilitated in zFP506 N66D than in wild-type z2FP574, and as for z2FP574 D66E, the oxidized and non-decarboxylated species would accumulate. In contrast to z2FP574 D66E, zFP506 N66D exhibited a considerably increased contribution of the red constituent to the absorbance spectra (Figure 2A). Mass spectra of the zFP506 N66D red chromopeptide indicated oxidation−decarboxylation at position 66 of a GFP-like structure; however, an oxidized and non-decarboxylated species was not detected, suggesting that these two reactions are tightly coupled in N66D. We also examined whether oxidation to an acylimine affects aspartate decarboxylation. Given that oxidation of the cgCP chromophore to an acylimine is not dependent on the nature of the first chromophore-forming amino acid (*9*), we expected that introduction of the A63D substitution into cgCP would not disturb its original oxidation pathway. The A63D mutant of cgCP exhibited an absorbance spectrum exactly the same as that of the wild-type protein (Figure 2B). MALDI-TOF mass spectra of the A63D chromopeptide contained two peaks at *m*/*z* 994.3 and 1038.3 (Figure 2 of the Supporting Information). The first peak is essentially the same as that observed for the wild-type chromopeptide (*9*), suggesting that aspartate within the cgCP A63D chromophore is oxidized and decarboxylated. The minor peak at *m*/*z* 1038.3 is consistent with the oxidized and non-decarboxylated intermediate. Hence, oxidation to an acylimine facilitates aspartate decarboxylation. In contrast, H62D substitution in a green fluorescent protein from *Dendronephthya* sp., which is deficient in additional oxidation to an acylimine, did not lead to aspartate decarboxylation (Table 3).

Recently, Verkhusha et al. (*17*) proposed that the red chromophore of DsRed and related chromoproteins is produced from the protonated form of a GFP-like intermediate absorbing at 408 nm. They also demonstrated that the green anionic form of a GFP-like chromophore absorbing at 480 nm is not an intermediate in the red chromophore synthesis, which had been suggested earlier. To study the maturation kinetics, we followed absorbance spectral changes, assuming that efficient fluorescence resonance energy transfer (FRET) between green and red species within the protein tetramers might contribute to fluorescence spectra (*17*). Indeed, a protonated GFP-like intermediate absorbing at 408 nm was detected during wild-type cgCP maturation (not shown). However, we did not detect a 408 nm intermediate upon z2FP574 maturation. In contrast to DsRed chromophore synthesis, maturation kinetics of wild-type z2FP574 (Figure 3A,B), and particularly that of the zFP506 N66D mutant (Figure 4A), definitely indicated the green GFP-like intermediate in the reaction producing the red chromophore. The isosbestic point at 514 nm in the course of the zFP506 N66D green-to-red transition indicated contributions from only two species. We further exploited the temperature sensitivity of the N66D green-to-red conversion in efforts to arrest the reaction at distinct stages and analyze the reaction products by mass spectrometry. According to mass spectra, the green-to-red reaction products of N66D mutant are deficient in decarboxylated-only or oxidized-only species. Thus, it is likely that oxidation and decarboxylation of Asp-66 occur via short-lived intermediates, making it difficult to detect them by the methods described above.

Figure 5 illustrates the proposed steps in oxidation−decarboxylation of the z2FP574 chromophore. The only facile decarboxylation known in organic chemistry is that of β-keto acids. The reaction proceeds via a high-energy carbanion intermediate that requires a stabilizer. Upon β-keto acid decarboxylation, the β-keto group stabilizes the negative charge of the carbanion. Enzymes use a variety of chemical tricks to provide stabilization. Some of them, in place of a β-keto group, form a Schiff base with the substrate, the positive charge of which potentiates stabilization of the carbanion (*20*−*22*). The z2FP574 chromophore also forms a Schiff base at the β-position to a carboxy group of the progenitor aspartate (Figure 5, structure **b**). The carbanion can also be efficiently stabilized by delocalization into the electron-accepting moiety of the intermediate green form of the chromophore (Figure 5, structures **d**−**f**). Unlike aspartate, the carbanion formed by glutamate within the z2FP574 D66E mutant cannot be stabilized in this way, which explains the lack of decarboxylated species in the minor red form of the D66E mutant.

In summary, we found the red fluorescence of z2FP574 to arise from chemical reactions, which are different from those reported for DsRed. The z2FP574 red species is produced from an anionic (green) form by a coupled oxidation−decarboxylation of a GFP-like chromophore. In contrast, the DsRed chromophore has been proposed to originate from oxidation of a protonated (blue) form of a GFP-like structure, an anionic green form assumed to be a dead-end product (*17*). These results imply that a green-to-red fluorescence transition of DsRed mutant E5, also known as a fluorescent timer (*23*), is not due to a direct conversion of green species into the red one but stems from an increasing level of FRET between green and red monomers within DsRed-E5 tetramers. Consequently, monomeric variants of DsRed-E5 would not be expected to undergo a green-to-red fluorescence transition that limits the DsRed-E5 potential to detecting promoter activity. If monomeric variants of z2FP574 or zFP506 N66D are obtained, it will be possible to use them as fluorescent tags for tracking the protein's fate upon aging.

ACKNOWLEDGMENT

We thank Dr. K. A. Lukyanov for providing us with the zFP506 and z2FP574 expression plasmids.

SUPPORTING INFORMATION AVAILABLE

SDS−PAGE analysis of the cgCP A63D polypeptide chain cleavage under different denaturing conditions (Figure 1) and a representative MALDI-TOF mass spectrum of the cgCP A63D chromopeptide (Figure 2). This material is available free of charge via the Internet at http://pubs.acs.org.

REFERENCES

1. Giepmans, B. N., Adams, S. R., Ellisman, M. H., and Tsien, R. Y. (2006) The fluorescent toolbox for assessing protein location and function, *Science 312*, 217−224.
2. Chudakov, D. M., Lukyanov, S., and Lukyanov, K. A. (2005) Fluorescent proteins as a toolkit for in vivo imaging, *Trends Biotechnol. 23*, 605−613.
3. Gross, L. A., Baird, G. S., Hoffman, R. C., Baldridge, K. K., and Tsien, R. Y. (2000) The structure of the chromophore within DsRed, a red fluorescent protein from coral, *Proc. Natl. Acad. Sci. U.S.A. 97*, 11990−11995.
4. Wall, M. A., Socolich, M., and Ranganathan, R. (2000) The structural basis for red fluorescence in the tetrameric GFP homolog DsRed, *Nat. Struct. Biol. 7*, 1133−1138.
5. Yarbrough, D., Wachter, R. M., Kallio, K., Matz, M. V., and Remington, S. J. (2001) Refined crystal structure of DsRed, a red fluorescent protein from coral, at 2.0-Å resolution, *Proc. Natl. Acad. Sci. U.S.A. 98*, 462−467.
6. Petersen, J., Wilmann, P. G., Beddoe, T., Oakley, A. J., Devenish, R. J., Prescott, M., and Rossjohn, J. (2003) The 2.0-Å crystal structure of eqFP611, a far red fluorescent protein from the sea anemone *Entacmaea quadricolor*, *J. Biol. Chem. 278*, 44626−44631.
7. Prescott, M., Ling, M., Beddoe, T., Oakley, A. J., Dove, S., Hoegh-Guldberg, O., Devenish, R. J., and Rossjohn, J. (2003) The 2.2 Å crystal structure of a pocilloporin pigment reveals a nonplanar chromophore conformation, *Structure 11*, 275−284.
8. Martynov, V. I., Maksimov, B. I., Martynova, N. Y., Pakhomov, A. A., Gurskaya, N. G., and Lukyanov, S. A. (2003) A purple-blue chromoprotein from *Goniopora tenuidens* belongs to the DsRed subfamily of GFP-like proteins, *J. Biol. Chem. 278*, 46288−46292.
9. Pakhomov, A. A., Pletneva, N. V., Balashova, T. A., and Martynov, V. I. (2006) Structure and reactivity of the chromophore of a GFP-like chromoprotein from *Condylactis gigantea*, *Biochemistry 45*, 7256−7264.
10. Labas, Y. A., Gurskaya, N. G., Yanushevich, Y. G., Fradkov, A. F., Lukyanov, K. A., Lukyanov, S. A., and Matz, M. V. (2002) Diversity and evolution of the green fluorescent protein family, *Proc. Natl. Acad. Sci. U.S.A. 99*, 4256−4261.
11. Pletneva, N., Pletnev, S., Tikhonova, T., Popov, V., Martynov, V., and Pletnev, V. (2006) Structure of a red fluorescent protein from *Zoanthus*, zRFP574, reveals a novel chromophore, *Acta Crystallogr. D62*, 527−532.
12. Gill, S. C., and von Hippel, P. H. (1989) Calculation of protein extinction coefficients from amino acid sequence data, *Anal. Biochem. 182*, 319−326.
13. Burmeister, W. P. (2000) Structural changes in a cryo-cooled protein crystal owing to radiation damage, *Acta Crystallogr. D56*, 328−341.
14. van Thor, J. J., Gensch, T., Hellingwerf, K. J., and Johnson, L. N. (2002) Phototransformation of green fluorescent protein with UV and visible light leads to decarboxylation of glutamate 222, *Nat. Struct. Biol. 9*, 37−41.
15. Pakhomov, A. A., Martynova, N. Y., Gurskaya, N. G., Balashova, T. A., and Martynov, V. I. (2004) Photoconversion of the chromophore of a fluorescent protein from *Dendronephthya* sp., *Biochemistry (Moscow, Russ. Fed.) 69*, 901−908.
16. Hoops, S., Sahle, S., Gauges, R., Lee, C., Pahle, J., Simus, N., Singhal, M., Xu, L., Mendes, P., and Kummer, U. (2006) COPASI: A COmplex PAthway SImulator, *Bioinformatics 22*, 3067−3074.
17. Verkhusha, V. V., Chudakov, D. M., Gurskaya, N. G., Lukyanov, S., and Lukyanov, K. A. (2004) Common pathway for the red chromophore formation in fluorescent proteins and chromoproteins, *Chem. Biol. 11*, 845−854.
18. Chan, M. C., Karasawa, S., Mizuno, H., Bosanac, I., Ho, D., Privé, G. G., Miyawaki, A., and Ikura, M. (2006) Structural characterization of a blue chromoprotein and its yellow mutant from the sea anemone *Cnidopus japonicus*, *J. Biol. Chem. 281*, 37813−37819.
19. Remington, S. J., Wachter, R. M., Yarbrough, D. K., Branchaud, B., Anderson, D. C., Kallio, K., and Lukyanov, K. A. (2005) zFP538, a yellow-fluorescent protein from *Zoanthus*, contains a novel three-ring chromophore, *Biochemistry 44*, 202−212.
20. Highbarger, L. A., Gerlt, J. A., and Kenyon, G. L. (1996) Mechanism of the reaction catalyzed by acetoacetate decarboxylase. Importance of lysine 116 in determining the pKa of active-site lysine 115, *Biochemistry 35*, 41−46.
21. Liu, D., Hwang, C. C., and Cook, P. F. (2002) Alternative substrates for malic enzyme: Oxidative decarboxylation of L-aspartate, *Biochemistry 41*, 12200−12203.
22. Begley, T. P., and Ealick, S. E. (2004) Enzymatic reactions involving novel mechanisms of carbanion stabilization, *Curr. Opin. Chem. Biol. 8*, 508−515.
23. Terskikh, A., Fradkov, A., Ermakova, G., Zaraisky, A., Tan, P., Kajava, A. V., Zhao, X., Lukyanov, S., Matz, M., Kim, S., Weissman, I., and Siebert, P. (2000) "Fluorescent timer": Protein that changes color with time, *Science 290*, 1585−1588.

BI700721X